Biallelic CAV1 null variants induce Congenital Generalized Lipodystrophy with achalasia Short title: CAV1, generalized lipodystrophy and achalasia

Asuman Nur Karhan, Jamila Zammouri, Martine Auclair, Emilie Capel, Feramuz Demir Apaydin, Fehmi Ateş, Marie-Christine Verpont, Jocelyne Magré, Bruno Fève, Olivier Lascols, et al.

Biallelic *CAV1* null variants induce Congenital Generalized Lipodystrophy with achalasia

Short title: *CAV1*, generalized lipodystrophy and achalasia

Asuman Nur Karhan[1*], Jamila Zammouri[2*], Martine Auclair[2], Emilie Capel[2], Feramuz Demir Apaydin[3], Fehmi Ates[4], Marie-Christine Verpont[5], Jocelyne Magré[6], Bruno Fève[2,7], Olivier Lascols[2,8], Yusuf Usta[1#], Isabelle Jéru[2,8#], Corinne Vigouroux[2,7,8#]

* and # equally contributing authors

[1] Department of Pediatric Gastroenterology, Hepatology and Nutrition, Mersin University Faculty of Medicine, Mersin, Turkey

[2] Sorbonne University, Inserm UMR_S938, Saint-Antoine Research Centre, Institute of Cardiometabolism and Nutrition, Paris, France

[3] Department of Radiology, Mersin University Faculty of Medicine, Mersin, Turkey

[4] Department of Gastroenterology, Mersin University Faculty of Medicine, Mersin, Turkey

[5] Sorbonne University, Inserm UMR_S1155, LUMIC, Tenon Imagery and Cytometry Platform, Paris, France

[6] Nantes University, CNRS, Inserm UMR_S1087, Institut du Thorax, F-44000 Nantes, France.

[7] Assistance Publique-Hôpitaux de Paris, Saint-Antoine University Hospital, National Reference Center for Rare Diseases of Insulin Secretion and Insulin Sensitivity (PRISIS), Department of Endocrinology, Diabetology and Reproductive Endocrinology, Paris, France

[8] Assistance Publique-Hôpitaux de Paris, Saint-Antoine University Hospital, Department of Molecular Biology and Genetics, Paris, France

Keywords: *CAV1*, lipodystrophy, autosomal recessive, achalasia, caveolae

Word count: 3673

Figures: 9**, Table:** 1**, Supplemental Table:** 1

Corresponding authors: Asuman Nur Karhan, Department of Pediatric Gastroenterology, Hepatology and Nutrition, Mersin University Faculty of Medicine, Mersin 33150, Turkey, asunurkar83@gmail.com, and Corinne Vigouroux, Sorbonne Université Médecine, Site Saint-Antoine, 27, rue Chaligny, 75571 Paris Cédex 12, France, corinne.vigouroux@inserm.fr

Funding sources: This work was supported by the French Ministry of Solidarity and Health, Assistance-Publique Hôpitaux de Paris, Sorbonne University, Centre National de la Recherche Scientifique, the Institut National de la Santé et de la Recherche Médicale (Inserm), and the Fondation pour la Recherche Médicale (EQU201903006878), France.

Disclosure summary: The authors have nothing to disclose

Abstract

***Objective**: CAV1* encodes caveolin-1, a major protein of plasma membrane microdomains called caveolae, involved in several signalling pathways. Caveolin-1 is also located at the adipocyte lipid droplet. Heterozygous pathogenic variants of *CAV1* induce rare heterogeneous disorders including pulmonary arterial hypertension and neonatal progeroid syndrome. Only one patient was previously reported with a *CAV1* homozygous pathogenic variant, associated with congenital generalized lipodystrophy (CGL3). We aimed to further delineate genetic transmission, clinical, metabolic and cellular characteristics of CGL3.

***Design/Methods**:* In a large consanguineous kindred referred for CGL, we performed next-generation sequencing, as well as clinical, imagery and metabolic investigations. We studied skin fibroblasts from the index case and the previously reported patient with CGL3.

***Results**:* Four patients, aged 8 months to 18 years, carried a new homozygous p.(His79Glnfs*3) *CAV1* variant. They all displayed generalized lipodystrophy since infancy, insulin resistance, low HDL-cholesterol and/or high triglycerides, but no pulmonary hypertension. Two patients also presented at the age of 15 and 18 years with dysphagia due to achalasia, and one patient had retinitis pigmentosa. Heterozygous parents and relatives (n=9) were asymptomatic, without any metabolic abnormality. Patients' fibroblasts showed a complete loss of caveolae and no protein expression of caveolin-1 and its caveolin-2 and cavin-1 partners. Patients' fibroblasts also displayed insulin resistance, increased oxidative stress and premature senescence.

***Conclusions**:* The *CAV1* null variant investigated herein leads to an autosomal recessive congenital lipodystrophy syndrome. Loss of caveolin-1 and/or caveolae induces specific manifestations including achalasia which requires specific management. Overlapping phenotypic traits between the different *CAV1*-related diseases require further studies.

INTRODUCTION

Caveolae are plasma membrane microdomains that act as signalling platforms in several cell types, including adipocytes, smooth muscle cells, endothelial cells and fibroblasts. The integral membrane protein caveolin-1, encoded by the *CAV1* gene, is required for caveolae formation and is the main protein component of caveolae. Caveolin-1 interacts, among others, with the insulin receptor and contributes to the compartmentalization of insulin signaling pathways (1). Caveolin-1 is also a fatty acid-binding protein able to translocate from the plasma membrane to the adipocyte lipid droplets, therefore contributing to the regulation of lipid storage (2,3). In addition, it plays a role in tumor suppression and oxidative stress-induced cellular senescence (4). Loss of caveolin-1 expression in mice induces several defects including progressive lipodystrophy with insulin resistance and hypertriglyceridemia (5,6), cardiomyopathy and pulmonary hypertension (7,8).

The phenotypic spectrum of the rare *CAV1* genetic defects in humans remains difficult to delineate. A single patient has been previously reported with a homozygous *CAV1* pathogenic variant. This patient was a young woman described with congenital generalized lipodystrophy (CGL), severe insulin-resistant diabetes, and hypertriglyceridemia, referred to as CGL3 (9). Heterozygous *CAV1* null variants, including nonsense and frameshift mutations, have been reported so far in ten patients with different phenotypes, *i.e.* partial lipodystrophy with neurological involvement (10), precocious and severe pulmonary arterial hypertension (11-13) and/or neonatal progeroid syndromes (14-16).

In the present study, we investigated a large consanguineous kindred referred for CGL and identified a novel homozygous *CAV1* frameshift variant in four affected young patients.

Besides variable insulin resistance-associated metabolic abnormalities, esophageal achalasia, leading to severe dysphagia, emerges as a specific comorbidity. One affected patient also displayed atypical retinitis pigmentosa. By studying cultured skin fibroblasts from the index case and from the previously reported patient with a homozygous *CAV1* nonsense variant (9), we show that CGL3 is associated with a complete loss of protein expression of caveolin-1 and its partners caveolin-2 and cavin-1, and with the absence of caveolae at the plasma membrane. Fibroblasts from patients also display insulin resistance, increased oxidative stress and premature senescence.

PATIENTS AND METHODS

Patients

This study includes nineteen individuals from a large Turkish consanguineous family investigated at Mersin University, Department of Pediatric Gastroenterology, Hepatology and Nutrition, Turkey. Genetic studies were performed in the Department of Molecular Biology and Genetics, and the disease features were reviewed in the French Reference Center for Rare Diseases of Insulin Secretion and Insulin Sensitivity (PRISIS), both at Assistance-Publique Hôpitaux de Paris, Saint-Antoine Hospital, Paris, France. Clinical and molecular studies, and skin biopsy were performed after full written informed consent, according to the Ethics Committee of Mersin University. The study was approved by a French institutional research ethics board (CPP Ile de France 5). Written informed consent for publication of their clinical details and/or clinical images was obtained from the patients' parents, from patients themselves when aged above 12, and from their relatives.

Genetic analyses

Exons and flanking intronic sequences of a panel of 23 genes involved in lipodystrophic and/or insulin resistance syndromes, including *CAV1*, were sequenced from genomic DNA in Patient 1, as described (17) **(Figure 1)**. Sanger sequencing was performed with the Big Dye Terminator v3.1 sequencing kit (Thermo Fisher Scientific, Waltham, MA, USA) after polymerase chain reaction. Data were analyzed on a 3500xL Dx device with the SeqScape v2.7 software (Thermo Fisher Scientific). *CAV1* variants were described based on the longest isoform (NM_001753.4) using Alamut 2.11 (Sophia Genetics, Switzerland) and Human Genome Variation Society guidelines.

Fibroblast cultures

Primary fibroblast cultures from Patient 1 were established after skin biopsy. Cultured fibroblasts from the previously reported patient with CGL3, carrying the homozygous *CAV1* p.Glu38* pathogenic variant (9), and from two non-obese, non-diabetic, normotensive women who underwent plastic surgery (18) were studied at similar passages. Cells were grown in DMEM low glucose with pyruvate (#31885049; Thermo Fisher Scientific) supplemented with 10% fetal bovine serum (D. Dutscher, Bernolsheim, France), 1% penicillin/streptomycin, and 2 mM glutamine (Invitrogen, Cergy-Pontoise, France).

Transmission electron microscopy

Cultured fibroblasts were fixed in 2.5% glutaraldehyde, 0.1M cacodylate buffer at 4°C, rinsed in 0.2M cacodylate, post-fixed in 1.5% potassium ferrocyanide 1% osmium tetroxide, dehydrated using graded alcohol series, then embedded in epoxy resin. Semi-fine sections (0.5 µm) were stained with toluidine blue. Ultrathin sections (70 nm) were contrasted with UranyLess and lead citrate (Delta Microscopies, France) and examined using an electron microscope (JEOL 2110 HC, Croissy, France) with a 2Kx2K Veleta CCD camera (Olympus,

Rungis, France).

Western blot

Protein expression studies were performed on whole cell extracts using antibodies described in **Supplemental Table 1**.

Cellular response to insulin

To measure their ability to bind insulin, fibroblasts were maintained for 16 hours in serum-free medium supplemented with 0.1% albumin (Sigma-Aldrich, Saint-Louis, MO, USA), then incubated with ^{125}I-insulin (0.3 ng/mL, PerkinElmer, Coutaboeuf, France) with or without unlabeled insulin (5.10^{-8}M) in Hepes buffer at pH 7.65, 15°C, for 5 hours. Radioactivity was measured in a gamma counter (PerkinElmer 2470 Wizard2) and results were normalized to protein content. Insulin effect on glycogen synthesis was evaluated by the incorporation of ^{14}C-glucose as previously described (19). Results were normalized to the protein content and expressed as a percentage of the basal value.

Oxidative Stress and Cellular Senescence

The production of reactive oxygen species (ROS) was assayed by quantifying the oxidation of 5-6-chloromethyl-2,7-dichlorodihydrofluorescein diacetate (CM-H_2DCFDA). The blue staining produced by hydrolysis of X-gal (5-bromo-4-chloro-3-indolyl-ß-Dgalactopyranoside) by senescence-activated-ß-galactosidase at pH 6.0 was used as a biomarker of cellular senescence, as previously described (20). The ratio of pH 6-to-pH 4 staining of blue X-gal was quantified at 630 nm.

Statistical analyses

GraphPad Prism software (GraphPad Software Inc., CA, USA) was used to calculate statistical significance with a threshold at $p<0.05$. Gaussian distribution was tested with Kolmogorov–Smirnov test. Differences between two groups were assessed by unpaired two-sample t-tests or Mann-Whitney tests and multiple comparisons between more than two groups were conducted by ANOVA with Bonferroni-test or Kruskal-Wallis test for post-hoc analysis. All data are means ± SEM of at least three independent experiments.

RESULTS

Identification of a novel *CAV1* pathogenic variant responsible for an autosomal recessive congenital generalized lipodystrophy syndrome

Patient 1, a 15-year-old girl from a large consanguineous Turkish family was referred for genetic investigation of CGL **(Figure 1)**. We identified a novel homozygous *CAV1* variant (NM_001753.4) : c.237_238del, p.(His79Glnfs*3) through sequencing of a panel of 23 genes involved in lipodystrophy and/or insulin resistance syndromes. This variant, confirmed by Sanger sequencing, was absent from the gnomAD and ExAC databases that list genetic variants from the general population, and is classified as pathogenic according to the American College of Medical Genetics and Genomics (ACMG) criteria (21). The deletion of 2 nucleotides in exon 3 leads to a shift in the reading frame. If the transcript is expressed, it is predicted to result in the synthesis of an abnormal form of caveolin-1, truncated in its oligomerization domain and deprived from its scaffolding and intra-membrane domains **(Figure 2)**. Sequencing of the gene panel did not reveal any other pathogenic variant. Patient 1 was thus diagnosed with CGL3.

The same *CAV1* variant was observed in the homozygous state in Patient 2, who was subsequently referred with similar symptoms, and in Patients 3 and 4, diagnosed with CGL after familial investigations. The parents of Patients 1 to 4 were asymptomatic. Genetic investigations, performed in seven of them, revealed that they were heterozygous carriers of

the variant. Unaffected siblings of the patients (n=8) were heterozygous for the variant or had a normal genotype.

This family thus showed an autosomal recessive transmission of CGL3 due to a novel p.(His79Glnfs*3) *CAV1* pathogenic variant **(Figures 1 and 2)**.

Phenotype of the disease

Table 1 summarizes the patients' main phenotypic features.

Patient 1

Patient 1 was referred at the age of 15 to Mersin University with difficulty in swallowing liquids and solids. She was born from first-cousin parents of Turkish origin, at term after an uneventful pregnancy, with a birth weight and height of 2800g and 48cm respectively. At examination, her height was 153 cm, BMI was 17.9, Tanner pubertal stage 5. She showed a triangular and acromegaloid face, with a generalized loss of fat sparing palms and soles, a taut and thin mottled skin with visible dermal vessels, extensive acanthosis nigricans in the armpits and groins, a prominent musculature, and enlarged hands and feet **(Figure 3A-C)**. She also complained about hirsutism, with secondary amenorrhea since the age of 14. The family noticed her dysmorphic facial and body appearance during early infancy. Although her linear growth was delayed with poor weight gain during infancy, she was described with a voracious appetite. She did not present with any skeletal deformity, joint contractures or muscular functional defect. No cognitive delay was observed and she had normal developmental milestones. Neurological examination was normal. Blood pressure was normal.

Laboratory parameters showed hypertriglyceridemia (5.4 mmol/L), low HDL-cholesterol (0.73 mmol/L), major fasting hyperinsulinemia (300 mIU/L) with normal glycemia (5 mmol/L) and HbA1c (5.8%). Liver tests and creatine kinase were normal as well as kidney and thyroid

function. Androgen levels were in the normal range. Serum luteinizing hormone (LH, 13.9 IU/L) was higher than follicle-stimulating hormone (FSH, 5.8 IU/L). Estradiol levels were in the normal range for the follicular phase. Calcemia and parathormone serum and urinary levels were normal, with decreased vitamin D level and bone mineral density (Z score -2.78 at lumbar spine).

Generalized lipoatrophy was confirmed by magnetic resonance imaging (MRI) **(Figure 4)**, and by very low leptin levels (0.3 ng/mL), also consistent with hyperphagia. MRI also revealed enlarged polycystic ovaries (**Figure 5)**. Electrocardiogram and echocardiogram, including estimated right ventricular systolic pressure, were normal. Liver steatosis was diagnosed with ultrasonography. Medical history, physical examination and results of metabolic investigations allowed the diagnosis of CGL. A treatment with metformin and medium-chain triglycerides was initiated.

Dysphagia was investigated with several procedures. Barium esophagogram series showed a dilated esophagus with a distal bird's beak deformity **(Figure 6A)**, and a severe stenosis of the distal esophagus was confirmed by endoscopy. High resolution esophageal manometry showed the absence of lower esophageal sphincter relaxation with increased integrated relaxation pressure (51 mmHg) and decreased peristalsis, consistent with esophagogastric junction outflow obstruction (22) **(Figure 6 B,C)**. Based on clinical, endoscopic, radiological and manometric findings, an early stage of achalasia was diagnosed. Peroral endoscopic myotomy (POEM) was performed leading to a significant relief in dysphagia-related symptoms.

Patient 2

Patient 2 was an 18-year-old cousin of Patient 1 **(Figure 1)** referred for difficulty in swallowing. Generalized lipodystrophy and mild dysmorphic features were present from early infancy. His symptoms and physical examination were very similar to those of Patient 1 **(Table 1, Figure**

3D). However, his metabolic abnormalities were milder, with low HDL-cholesterol but normal triglyceridemia. Although glucose tolerance was normal, normal-to-high 2h-postprandial insulin (45.8 mIU/L, N: 4-52.5 at T120 min after oral glucose tolerance test) (23) and C-peptide levels (8.32 µg/L, N: 1.1-4.4) suggested insulin resistance. Blood pressure, cardiac examination including echocardiography were normal, as well as liver, renal and thyroid function, and testosterone and FSH levels. Type 2 achalasia, diagnosed upon radiological, endoscopic and manometric findings **(Figure 6 D-F)**, was successfully treated by POEM. Patient 2 also complained of trouble seeing at night for two years. Although neurological examination and ophthalmological fundus analysis were normal, optical coherence tomography (OCT) revealed bilateral loss of ellipsoid line and atrophy of the retinal pigment epithelium, and defective outer limiting membrane in the left eye, suggesting atypical retinitis pigmentosa.

Patient 3 and Patient 4

Patient 3, a 10-year-old girl, and Patient 4, an 8-month-old girl, were investigated during the systematic familial screening **(Figure 1)**. As Patients 1 and 2, they were born from consanguineous parents, at term after normal pregnancies, with normal birth weight and height. Their linear growth was delayed and they presented with a dysmorphic appearance and generalized lipoatrophy, which were noticed by the family during early infancy **(Figure 3 E,F)**. Their physical examination was otherwise normal. They both achieved normal developmental milestones. Laboratory investigations revealed increased levels of triglycerides and insulin, and decreased HDL-cholesterol **(Table 1)**.

Patients' relatives

Relatives of Patients 1 to 4 (n=15) **(Figure 1)** had no complaint and did not show any sign of lipodystrophy. Their anthropometric measurements and physical examination were normal,

except for the older brother of Patient 1 who presented with a mild mental retardation of unknown origin. Their laboratory evaluation including full blood count, fasting glucose and insulin, HbA1c, liver function tests and serum lipids, were normal.

Homozygous *CAV1* p.(His79Glnfs*3) and p.(Glu38*) pathogenic variants induce a loss of protein expression of caveolin-1, caveolin-2 and cavin-1, and a loss of caveolae formation in patients' fibroblasts

We compared cultured fibroblasts from Patient 1 and from the previously reported patient with CGL due to the homozygous p.(Glu38*) *CAV1* pathogenic variant (9), to those from controls. The p.(His79Glnfs*3) and the previously described p.(Glu38*) *CAV1* pathogenic variants predict to interrupt the caveolin-1 aminoacid sequence at the N-terminal part of the protein, proximally to its scaffolding and intra-membrane domains (24) **(Figure 2)**. As expected, we show that, similarly to the fibroblasts carrying the homozygous *CAV1* p.(Glu38*) variant (9), cells from Patient 1 with the novel *CAV1* p.(His79Glnfs*3) variant do not exhibit detectable expression of caveolin-1 **(Figure 7A)**. We evaluated the protein expression of caveolin-2 and cavin-1, which are binding partners of caveolin-1. We show that caveolin-2 and cavin-1 protein levels are strongly decreased in patients' cells **(Figure 7A).** Notably, pathogenic variants in *CAVIN1* (previously referred to as *PTRF*), encoding cavin-1, lead to a form of CGL previously associated with achalasia (25). As expected from the major role of caveolin-1 and cavin-1 for caveolae formation, electron microscopy shows that caveolae, abundant in control cells, are completely absent in fibroblasts from patients with *CAV1* null variants **(Figure 7B).**

Homozygous *CAV1* null variants impair insulin signaling

We then investigated the insulin-mediated activation of proximal signalling intermediates from the metabolic and mitogenic insulin pathways (*i.e*, IRß, IRS1, AKT, and ERK1/2) and show

that it is strongly impaired in fibroblasts from patients with *CAV1* null variants **(Figure 8A)**. In addition, the effect of insulin on its distal signalling, as evaluated by glycogen synthesis, is also severely inhibited in patients' cells **(Figure 8B)**. Although the total amount of insulin receptors is not significantly decreased in whole protein extracts from patients' cells **(Figure 8A)**, the absence of caveolae, which are normally enriched at the plasma membrane with insulin receptors (1), could impair the initiation of the insulin signal. To test this hypothesis, we evaluated the capacity of fibroblasts to bind insulin, and showed that it was decreased by ~ 20% in cells bearing *CAV1* null variants as compared to control cells **(Figure 8C).** These results suggest that the loss of caveolae could contribute, in part, to the insulin resistance observed in cells from patients carrying *CAV1* null pathogenic variants.

Homozygous *CAV1* null variants increase oxidative stress and senescence in fibroblasts

Caveolin-1 has been shown to modulate oxidative stress-induced cellular senescence (4), a pathway which has been involved in lipodystrophic diseases (26). We thus aimed to evaluate the effects of *CAV1* pathogenic variants on the production of reactive oxygen species (ROS) and on cellular senescence. Patients' fibroblasts, as compared to control cells, display a major increase in oxidative stress **(Figure 9A)**, as well as elevated levels of senescence markers **(Figure 9B)**, and increased senescence-activated-β-galactosidase activity **(Figure 9 C,D)**.

DISCUSSION

We report here a novel homozygous null pathogenic variant in *CAV1* in four patients with CGL3, and show the autosomal recessive transmission of the disease in a large consanguineous family. This study adds important phenotypic data, since CGL3 was previously described in only one patient (9). By revealing the consequences of *CAV1* loss-of-function in patients' cells, this study also highlights the involvement of caveolin-1 and caveolae in cellular insulin

response, oxidative stress and cellular senescence, that could contribute to specific clinical manifestations.

Insulin resistance and related signs, including acanthosis nigricans, prominent veins, muscular hypertrophy, hypertriglyceridemia, low HDL-cholesterol, hirsutism and/or polycystic ovary syndrome, and hepatic steatosis, are consistently associated with lipodystrophy syndromes (27). These manifestations, together with generalized lipoatrophy, were present in the previously described patient with CGL3 (9) as well as, with variable severity, in the affected patients from this study. As previously described in other CGL subtypes, with the exception of CGL2 (9, 28), lipoatrophy only spared mechanical adipose tissue (from palms, plantar and retro-orbital regions) and bone marrow fat. It can be hypothesized that different adipose tissue depots, which have specific developmental origin and gene expression, could be differently impacted by CGL-associated pathogenic variants (29).

Lipodystrophy-associated insulin resistance was shown to result, at least in part, from defective adipocyte lipid storage and leptin deficiency leading to cellular lipotoxicity (30). Our studies in patients' fibroblasts suggest that deficient caveolin-1 and cavin-1 protein expression and/or the complete absence of caveolae could also directly contribute to insulin resistance.

The CGL3 phenotype was previously associated with short stature, hypocalcemia, osteopenia and megaesophagus (9), but whether these signs were due to the homozygous *CAV1* null variant remained elusive. We show that achalasia, diagnosed at age 15 and 18 in two affected patients, should be considered as a main complication of CGL3 requiring careful investigations and specific management. Endoscopic myotomy was successful in the two affected patients, and avoided invasive surgical procedures. Three affected patients from this study had short stature,

and one patient (Patient 3) had a height percentile under 25th, contrasting with the accelerated growth frequently described in patients with CGL1 and CGL2, due to *AGPAT2* or *BSCL2* pathogenic variants, respectively (27). Whether this could be due to the severe impairment of insulin-activated mitogenic signalling pathways linked to the loss of caveolae requires further studies. The four patients did not present with any clinical bone or joint abnormality. However, we did observe osteopenia in two of the investigated patients, with a Z-score below -2.5 at the lumbar spine level, contrasting with the increased bone density usually observed in patients with CGL1 or CGL2 (27,31). Interestingly, osteopenia was confirmed by DEXA at the age of 21 in the previously described patient with CGL3, with a lumbar spine Z-score of -3 (Dr Chong Kim, personal communication). The decreased bone mass observed in Patient 1 and Patient 2 was not explained by vitamin D nor sex steroid hormone levels. In addition, in contrast to hypocalcemia with hypercalciuria observed in the previously reported patient (9), and in caveolin-1 knockout mice (32), serum and urinary calcium were normal in patients from this study. Detailed investigations of calcium homeostasis remains to be performed in CGL3.

The biallelic pathogenic variants responsible for CGL3, located in exon 2 and proximal exon 3 of *CAV1*, lead to similar phenotypes associated with a loss of protein expression of caveolin-1 and of its partner caveolin-2 (9, this study). Our results show that these variants also strongly inhibit cavin-1 protein expression, and lead to a complete loss of caveolae at the plasma membrane of patients' fibroblasts. Heterozygous subjects were asymptomatic, suggesting that half amount of functional caveolin-1 is sufficient to avoid any specific pathological consequences. In contrast, *CAV1* variants affecting the C-terminal domain of the protein, were reported as pathogenic in the heterozygous state and lead to rare but heterogeneous diseases **(Figure 2)** that may result from different pathophysiological mechanisms. Functional studies of the *CAV1* p.(Leu159Serfs*22) variant, responsible for autosomal dominant pulmonary

arterial hypertension, showed that the mRNA and protein expression of the mutated allele is preserved, and that the resulting abnormal protein could act *via* a dominant-negative effect on the trafficking of caveolin-1 to the plasma membrane (11-13). The *CAV1* p.(Phe160*) variant, reported in one patient with a neonatal complex progeroid syndrome associated with pulmonary artery hypertension and lipodystrophy, was also shown to be transcribed, without increased RNA degradation (14,15). In accordance, caveolae were present at the cell surface of the patient's fibroblasts, but caveolin-1 oligomers displayed decreased stability and weakened interactions with cavin-1 (14-16).

Cavin-1, encoded by the *CAVIN1* gene, is a caveolin-1-interacting protein, which, like caveolin-1, stabilizes caveolae structures. Cavin-1 is located at adipocyte lipid droplets, and contributes to the adipocyte differentiation process (2,3,18,33). Biallelic *CAVIN1* pathogenic variants are responsible for CGL4, a form of CGL also characterized by skeletal and/or cardiac muscular dystrophy (30,31), with achalasia in some patients (25,34,35). Achalasia is due to the dysfunction of nitrergic inhibitory motor neurones that innervate the circular smooth muscle of the distal esophagus, resulting in impaired relaxation of lower esophageal sphincter (36). We and others have previously shown that CGL4-related *CAVIN1* pathogenic variants severely impair cavin-1 and caveolin expression, as well as caveolae formation (18,35,37). Since caveolae have been shown to regulate calcium homeostasis and excitation-contraction coupling in smooth muscle (38,39), their deficiency could promote the development of uncontrolled esophageal contractions, that may evolve to achalasia. Oxidative stress could also contribute to achalasia, as reported in the Triple A (alacrima – achalasia – adrenal insufficiency) syndrome (OMIM 231550) (40). In addition, oxidative stress and/or premature senescence could participate in the pathophysiology of lipodystrophy (26,27,30,41).

Patient 2 from this study was diagnosed with atypical retinitis pigmentosa. Interestingly, caveolin-1 has been shown to modulate retinal neuroprotective signalling (42,43), and retinitis pigmentosa was reported in two patients with a syndrome of partial lipodystrophy, congenital cataracts, and neurological abnormalities, due to the heterozygous *CAV1* p.(Lys135Argfs*4) variant (10). However, ophthalmological fundus examination did not show any sign of retinitis pigmentosa in the previously described patient with CGL3, investigated at the age of 26 (9, and Dr Chong Kim, personal communication). Whether this sign could be due to CGL3-associated *CAV1* variants remains hypothetical. Dysmorphic features and/or mottled skin were observed in the affected patients from this study and in the two patients reported with neonatal premature ageing syndrome due to *de novo CAV1* variants (14,15) **(Figure 2)**, but no other progeroid sign was observed in patients with CGL3. Although right heart catheterization was not performed, clinical examination and echocardiography did not reveal any sign of pulmonary arterial hypertension in patients with CGL3.

Other phenotypic studies are required to better delineate the clinical relationships between the different *CAV1*-related diseases, due to loss-of-function or dominant negative mechanisms. However, in addition to careful metabolic monitoring, we suggest that gastrointestinal, cardiac, ophthalmological and neurological evaluation should also be included in the follow-up of patients with CGL3.

ACKNOWLEDGEMENTS

The authors thank the patients and their families for their participation in this study. They thank Audrey Geeverding and Michael Trichet from Sorbonne University, Department of Electron Microscopy, Paris-Seine Biology Institute, Paris, France for expert advice and help with electron microscopy, Dr Chong Kim, Department of Pediatrics, da Criança Institute, University

of Sao Paulo, Brazil for updated clinical data of the previously reported patient with CGL3, and Dr Sonja Janmaat, from the National Reference Center for Rare Diseases of Insulin Secretion and Insulin Sensitivity (PRISIS), Assistance Publique-Hôpitaux de Paris, France, for editorial assistance. Corinne Vigouroux is a member of the European Reference Network on Rare Endocrine Conditions – Project ID No 739527.

DISCLOSURE

The authors declare that there is no conflict of interest that could be perceived as prejudicing the impartiality of the research reported. This study was supported by institutional fundings from Inserm, Sorbonne Université, Centre National de la Recherche Scientifique, and Assistance-Publique Hôpitaux de Paris, and by Fondation pour la Recherche Médicale (grant number EQU201903007868).

REFERENCES

1. Saltiel AR & Pessin JE. Insulin signaling in microdomains of the plasma membrane. *Traffic* 2003 **4** 711-716.

2. Le Lay S, Hajduch E, Lindsay MR, Le Liepvre X, Thiele C, Ferre P, Parton RG, Kurzchalia T, Simons K & Dugail I. Cholesterol-induced caveolin targeting to lipid droplets in adipocytes: a role for caveolar endocytosis. *Traffic* 2006 **7** 549-561.

3. Hodges BD & Wu CC. Proteomic insights into an expanded cellular role for cytoplasmic lipid droplets. *J Lipid Res* 2010 **51** 262-273.

4. Zou H, Stoppani E, Volonte D & Galbiati F. Caveolin-1, cellular senescence and age-related diseases. *Mech Ageing Dev* 2011 **132** 533-542.

441 5. Razani B, Combs TP, Wang XB, Frank PG, Park DS, Russell RG, Li M, Tang B, Jelicks
442 LA, Scherer PE, *et al*. Caveolin-1-deficient mice are lean, resistant to diet-induced obesity, and
443 show hypertriglyceridemia with adipocyte abnormalities. *J Biol Chem* 2002 **277** 8635-8647.
444 6. Le Lay S, Blouin CM, Hajduch E & Dugail I. Filling up adipocytes with lipids. Lessons
445 from caveolin-1 deficiency. *Biochim Biophys Acta* 2009 **1791** 514-518.
446 7. Drab M, Verkade P, Elger M, Kasper M, Lohn M, Lauterbach B, Menne J, Lindschau
447 C, Mende F, Luft FC, *et al*. Loss of caveolae, vascular dysfunction, and pulmonary defects in
448 caveolin-1 gene-disrupted mice. *Science* 2001 **293** 2449-2452.
449 8. Zhao YY, Liu Y, Stan RV, Fan L, Gu Y, Dalton N, Chu PH, Peterson K, Ross J Jr &
450 Chien KR. Defects in caveolin-1 cause dilated cardiomyopathy and pulmonary hypertension in
451 knockout mice. *Proc Natl Acad Sci USA* 2002 **99** 11375-11380.
452 9. Kim CA, Delepine M, Boutet E, El Mourabit H, Le Lay S, Meier M, Nemani M, Bridel
453 E, Leite CC, Bertola DR, *et al.* Association of a homozygous nonsense caveolin-1 mutation
454 with Berardinelli-Seip congenital lipodystrophy. *J Clin Endocrinol Metab* 2008 **93** 1129-1134.
455 10. Cao H, Alston L, Ruschman J & Hegele RA. Heterozygous *CAV1* frameshift mutations
456 (MIM 601047) in patients with atypical partial lipodystrophy and hypertriglyceridemia. *Lipids*
457 *Health Dis* 2008 **7** 3.
458 11. Austin ED, Ma L, LeDuc C, Berman Rosenzweig E, Borczuk A, Phillips JA, 3rd,
459 Palomero T, Sumazin P, Kim HR, Talati MH, *et al.* Whole exome sequencing to identify a
460 novel gene (caveolin-1) associated with human pulmonary arterial hypertension. *Circ*
461 *Cardiovasc Genet* 2012 **5** 336-343.
462 12. Marsboom G, Chen Z, Yuan Y, Zhang Y, Tiruppathi C, Loyd JE, Austin ED, Machado
463 RF, Minshall RD, Rehman J, *et al.* Aberrant caveolin-1-mediated Smad signaling and
464 proliferation identified by analysis of adenine 474 deletion mutation (c.474delA) in patient

fibroblasts: a new perspective on the mechanism of pulmonary hypertension. *Mol Biol Cell* 2017 **28** 1177-1185.

13. Copeland CA, Han B, Tiwari A, Austin ED, Loyd JE, West JD & Kenworthy AK. A disease-associated frameshift mutation in caveolin-1 disrupts caveolae formation and function through introduction of a de novo ER retention signal. *Mol Biol Cell* 2017 **28** 3095-3111.

14. Garg A, Kircher M, Del Campo M, Amato RS, Agarwal AK & University of Washington Center for Mendelian G. Whole exome sequencing identifies de novo heterozygous *CAV1* mutations associated with a novel neonatal onset lipodystrophy syndrome. *Am J Med Genet A* 2015 **167A** 1796-1806.

15. Schrauwen I, Szelinger S, Siniard AL, Kurdoglu A, Corneveaux JJ, Malenica I, Richholt R, Van Camp G, De Both M, Swaminathan S, *et al.* A Frame-Shift Mutation in *CAV1* Is Associated with a Severe Neonatal Progeroid and Lipodystrophy Syndrome. *PLoS One* 2015 **10** e0131797.

16. Han B, Copeland CA, Kawano Y, Rosenzweig EB, Austin ED, Shahmirzadi L, Tang S, Raghunathan K, Chung WK & Kenworthy AK. Characterization of a caveolin-1 mutation associated with both pulmonary arterial hypertension and congenital generalized lipodystrophy. *Traffic* 2016 **17** 1297-1312.

17. Sollier C, Capel E, Aguilhon C, Smirnov V, Auclair M, Douillard C, Ladsous M, Defoort-Dhellemmes S, Gorwood J, Braud L, *et al.* LIPE-related lipodystrophic syndrome: clinical features and disease modeling using adipose stem cells. *Eur J Endocrinol* 2021 **184** 155-168.

18. Salle-Teyssieres L, Auclair M, Terro F, Nemani M, Elsayed SM, Elsobky E, Lathrop M, Delepine M, Lascols O, Capeau J, *et al.* Maladaptative Autophagy Impairs Adipose Function in Congenital Generalized Lipodystrophy due to Cavin-1 Deficiency. *J Clin Endocrinol Metab* 2016 **101** 2892-2904.

19. Thauvin-Robinet C, Auclair M, Duplomb L, Caron-Debarle M, Avila M, St-Onge J, Le Merrer M, Le Luyer B, Heron D, Mathieu-Dramard M, *et al.* PIK3R1 mutations cause syndromic insulin resistance with lipoatrophy. *Am J Hum Genet* 2013 **93** 141-149.

20. Le Dour C, Schneebeli S, Bakiri F, Darcel F, Jacquemont ML, Maubert MA, Auclair M, Jeziorowska D, Reznik Y, Bereziat V, *et al.* A homozygous mutation of prelamin-A preventing its farnesylation and maturation leads to a severe lipodystrophic phenotype: new insights into the pathogenicity of nonfarnesylated prelamin-A. *J Clin Endocrinol Metab* 2011 **96** E856-862.

21. Richards S, Aziz N, Bale S, Bick D, Das S, Gastier-Foster J, Grody WW, Hegde M, Lyon E, Spector E, *et al.* Standards and guidelines for the interpretation of sequence variants: a joint consensus recommendation of the American College of Medical Genetics and Genomics and the Association for Molecular Pathology. *Genet Med* 2015 **17** 405-424.

22. Yadlapati R, Kahrilas PJ, Fox MR, Bredenoord AJ, Prakash Gyawali C, Roman S, Babaei A, Mittal RK, Rommel N, Savarino E, *et al.* Esophageal motility disorders on high-resolution manometry: Chicago classification version 4.0((c)). *Neurogastroenterol Motil* 2021 **33** e14058.

23. Chevenne D, Léger J, Levy-Marchal C, Noel M, Collin D, Czernichow P, Porquet D. Proinsulin and specific insulin responses to an oral glucose tolerance test in a healthy population. *Diabetes Metab* 1998 **24** 260-261.

24. Ariotti N, Rae J, Leneva N, Ferguson C, Loo D, Okano S, Hill MM, Walser P, Collins BM & Parton RG. Molecular Characterization of Caveolin-induced Membrane Curvature. *J Biol Chem* 2015 **290** 24875-24890.

25. van der Pol RJ, Benninga MA, Magre J, Van Maldergem L, Rotteveel J, van der Knaap MS & de Meij TG. Berardinelli-Seip syndrome and achalasia: a shared pathomechanism? *Eur J Pediatr* 2015 **174** 975-980.

515 26. Vigouroux C, Caron-Debarle M, Le Dour C, Magre J & Capeau J. Molecular
516 mechanisms of human lipodystrophies: from adipocyte lipid droplet to oxidative stress and
517 lipotoxicity. *Int J Biochem Cell Biol* 2011 **43** 862-876.
518 27. Garg A. Lipodystrophies. *Am J Med* 2000 **108** 143-152.
519 28. Patni N, Garg A. Congenital generalized lipodystrophies--new insights into metabolic
520 dysfunction. *Nat Rev Endocrinol* 2015 **11** 522-534.
521 29. Billon N, Dani C. Developmental origins of the adipocyte lineage: new insights from
522 genetics and genomics studies. *Stem Cell Rev Rep* 2012 **8** 55-66.
523 30. Semple RK, Savage DB, Cochran EK, Gorden P & O'Rahilly S. Genetic syndromes of
524 severe insulin resistance. *Endocr Rev* 2011 **32** 498-514.
525 31. Lima JG, Nobrega LHC, Lima NN, Dos Santos MCF, Baracho MFP, Bandeira F,
526 Capistrano L, Freire Neto FP & Jeronimo SMB. Bone Density in Patients With Berardinelli-
527 Seip Congenital Lipodystrophy Is Higher in Trabecular Sites and in Type 2 Patients. *J Clin*
528 *Densitom* 2018 **21** 61-67.
529 32. Cao G, Yang G, Timme TL, Saika T, Truong LD, Satoh T, Goltsov A, Park SH, Men
530 T, Kusaka N, *et al.* Disruption of the caveolin-1 gene impairs renal calcium reabsorption and
531 leads to hypercalciuria and urolithiasis. *Am J Pathol* 2003 **162** 1241-1248.
532 33. Palacios-Ortega S, Varela-Guruceaga M, Milagro FI, Martinez JA & de Miguel C.
533 Expression of Caveolin 1 is enhanced by DNA demethylation during adipocyte differentiation.
534 status of insulin signaling. *PLoS One* 2014 **9** e95100.
535 34. Hayashi YK, Matsuda C, Ogawa M, Goto K, Tominaga K, Mitsuhashi S, Park YE,
536 Nonaka I, Hino-Fukuyo N, Haginoya K, *et al.* Human PTRF mutations cause secondary
537 deficiency of caveolins resulting in muscular dystrophy with generalized lipodystrophy. *J Clin*
538 *Invest* 2009 **119** 2623-2633.

539 35. Rajab A, Straub V, McCann LJ, Seelow D, Varon R, Barresi R, Schulze A, Lucke B,
540 Lutzkendorf S, Karbasiyan M, *et al.* Fatal cardiac arrhythmia and long-QT syndrome in a new
541 form of congenital generalized lipodystrophy with muscle rippling (CGL4) due to PTRF-
542 CAVIN mutations. *PLoS Genet* 2010 **6** e1000874.
543 36. Boeckxstaens GE. The lower oesophageal sphincter. *Neurogastroenterol Motil* 2005 **17**
544 **Suppl 1** 13-21.
545 37. Liu L, Brown D, McKee M, Lebrasseur NK, Yang D, Albrecht KH, Ravid K & Pilch
546 PF. Deletion of Cavin/PTRF causes global loss of caveolae, dyslipidemia, and glucose
547 intolerance. *Cell Metab* 2008 **8** 310-317.
548 38. Taggart MJ. Smooth muscle excitation-contraction coupling: a role for caveolae and
549 caveolins? *News Physiol Sci* 2001 **16** 61-65.
550 39. Parton RG & del Pozo MA. Caveolae as plasma membrane sensors, protectors and
551 organizers. *Nat Rev Mol Cell Biol* 2013 **14** 98-112.
552 40. Storr HL, Kind B, Parfitt DA, Chapple JP, Lorenz M, Koehler K, Huebner A & Clark
553 AJ. Deficiency of ferritin heavy-chain nuclear import in triple a syndrome implies nuclear
554 oxidative damage as the primary disease mechanism. *Mol Endocrinol* 2009 **23** 2086-2094.
555 41. Sollier C, Vatier C, Capel E, Lascols O, Auclair M, Janmaat S, Feve B, Jeru I &
556 Vigouroux C. Lipodystrophic syndromes: From diagnosis to treatment. *Ann Endocrinol (Paris)*
557 2020 **81** 51-60.
558 42. Reagan A, Gu X, Hauck SM, Ash JD, Cao G, Thompson TC & Elliott MH. Retinal
559 Caveolin-1 Modulates Neuroprotective Signaling. *Adv Exp Med Biol* 2016 **854** 411-418.
560 43. Gu X, Reagan AM, McClellan ME & Elliott MH. Caveolins and caveolae in ocular
561 physiology and pathophysiology. *Prog Retin Eye Res* 2017 **56** 84-106.
562 44. Tanner JM. Normal growth and techniques of growth assessment. *Clin Endocrinol*
563 *Metab* 1986 **15** 411-451.

FIGURE LEGENDS

Figure 1. Genealogical tree of the studied family

Patients 1 to 4, diagnosed with congenital generalized lipodystrophy and homozygous *CAV1* p.(His79Glnfs*3) variant (M/M) are depicted by filled symbols. Half-filled symbols (heterozygous subjects, +/M), and patients with normal genotype (+/+) were not affected by the disease. Patient 1 (P1, arrow) is the index case.

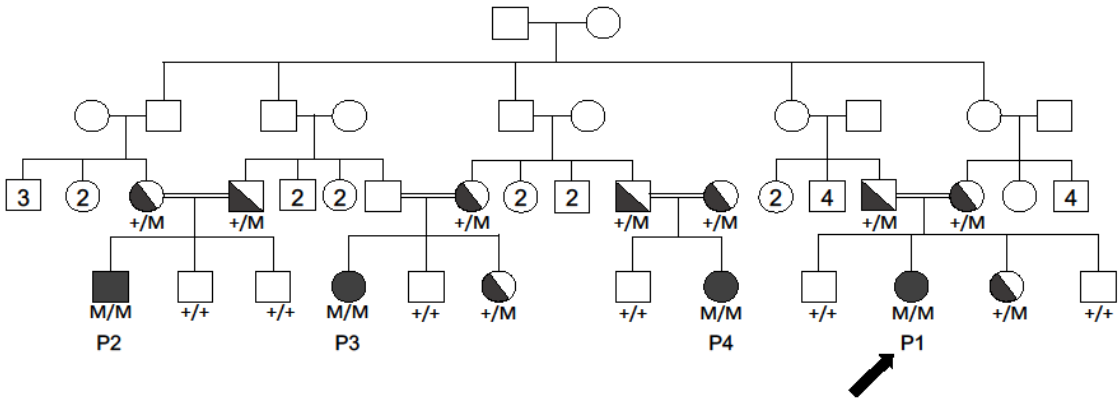

Figure 2. Schematic representation of *CAV1* gene and caveolin-1 protein

CAV1 pathogenic variants (NM_001753.4) identified in this study or previously reported (9-11, 14, 15) are indicated, with the corresponding phenotypes. OD: oligomerisation domain, CSD: caveolin-scaffolding domain

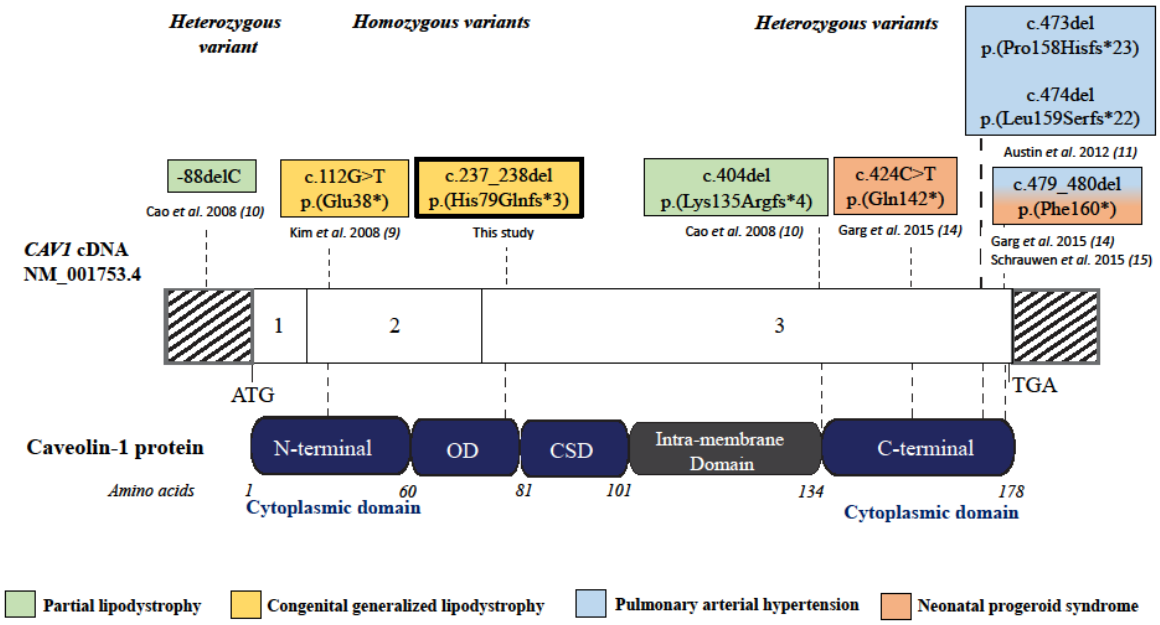

Figure 3. Photographs from patients with Congenital Generalized Lipodystrophy due to the novel *CAV1* p.(His79Glnfs*3) homozygous pathogenic variant

Photographs from Patient 1 (A-C), Patient 2 (D), Patient 3 (E), and Patient 4 (F) are shown. Triangular face with empty cheeks, and generalized lipoatrophy are observed in all patients. Muscular hypertrophy is visible in Patients 1-3. Photographs from Patient 1 also show mottled skin (A-C), acromegaloid features (A), and acanthosis nigricans (B).

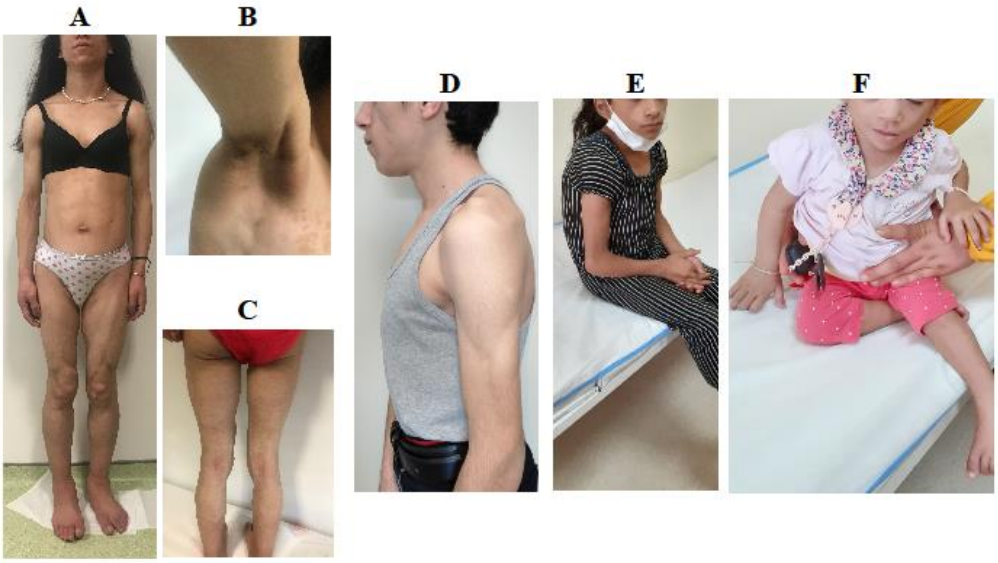

Figure 4. Magnetic resonance imaging of Patient 1 showing generalized lipoatrophy

Magnetic resonance T1-weighted images without fat suppression of Patient 1 and of an age, sex, and ethnically-matched control subject are shown.

Brain/cranial (A,B) and abdomen (C) axial images, and pelvis coronal images (D,E) of Patient 1 show that lipoatrophy is generalized, sparing only periorbital and bone marrrow regions. Hepatic steatosis and muscular hypertrophy are also visible.

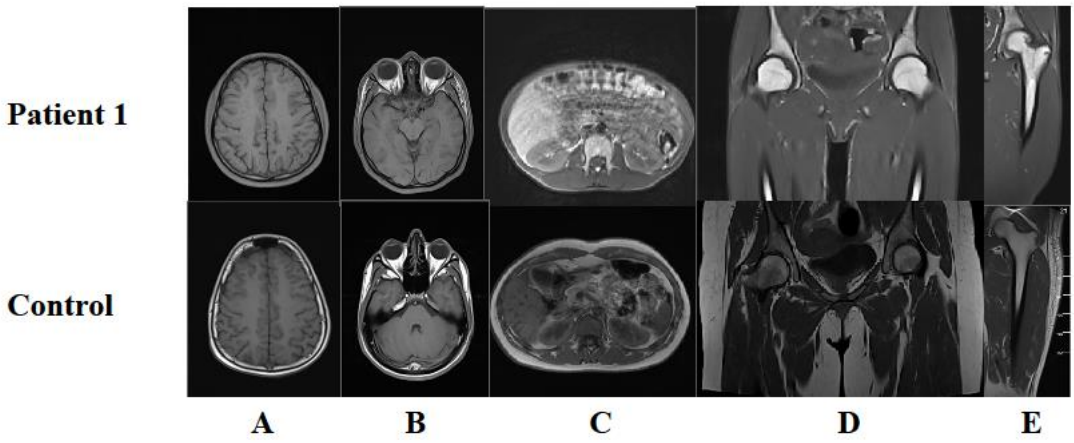

Figure 5. Magnetic resonance imaging of Patient 1 showing enlarged polycystic ovaries

Magnetic resonance T1-weighted coronal images of Patient 1, showing polycystic right (A) and left (B) ovaries of enlarged size (20 x 15 x 39 mm and 37 x 35 x 30 mm, respectively) (arrows).

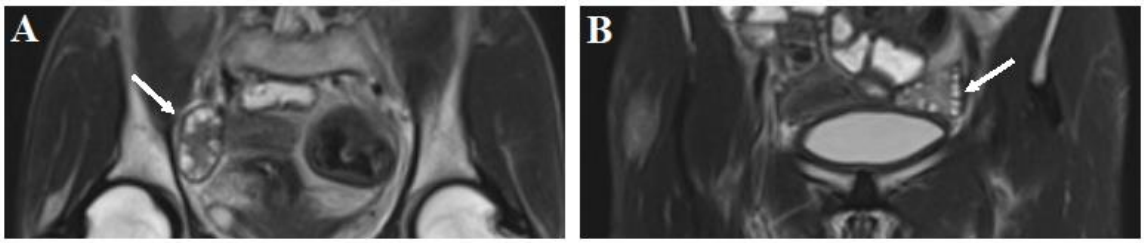

Figure 6. Barium esophagogram series and high-resolution manometry showing achalasia in Patient 1 and Patient 2

Barium esophagogram series in Patient 1 (A) and Patient 2 (D, E). Arrows show the bird's beak deformity at the distal part of esophagus (A, D) with dilated esophageal body (E).

High-resolution manometry, showing a pressure topography during a swallow, in a control subject (B), Patient 1 (C) and Patient 2 (F). The horizontal axis refers to time, and the vertical axis to length along the esophagus, with the lower esophageal sphincter (LES) depicted below. The pressure magnitude, encoded in color (blue, green, yellow, red from low to high pressure), is shown along the horizontal line. In a control subject, the pressure topography graph during a swallow shows a normal distal propagation of esophageal peristalsis, with LES relaxation over time (B). Weak peristalsis in Patient 1 defines esophagogastric junction outflow obstruction (C). A continuous high pressure without LES relaxation allows the diagnosis of Type 2 achalasia in Patient 2 (F).

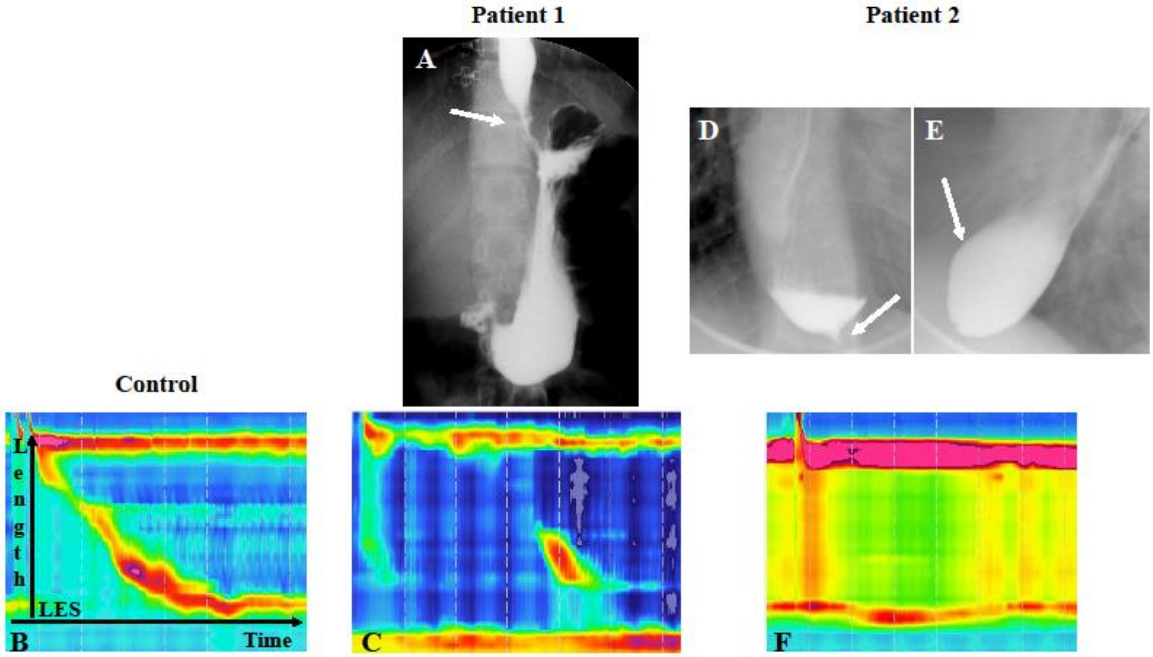

Figure 7. **Homozygous *CAV1* p.(His79Glnfs*3) and p.(Glu38*) pathogenic variants induce a loss of protein expression of caveolin-1, caveolin-2 and cavin-1, and a loss of caveolae formation in patients' fibroblasts**

(A) Protein expression of caveolin-1, caveolin-2 and cavin-1 in fibroblasts from controls, from Patient 1, carrying the *CAV1* p.(His79Glnfs*3) homozygous pathogenic variant, and from the patient previously described with a homozygous *CAV1* p.(Glu38*) variant responsible for CGL3 (9). Representative images of Western blots performed in triplicate are shown. Tubulin is used as an index of the cellular protein level. Numbers on the left correspond to the expected protein molecular weight. (B) Representative images of electron microscopy showing caveolae at the plasma membrane of control fibroblasts (arrows), which were completely absent in patients' cells.

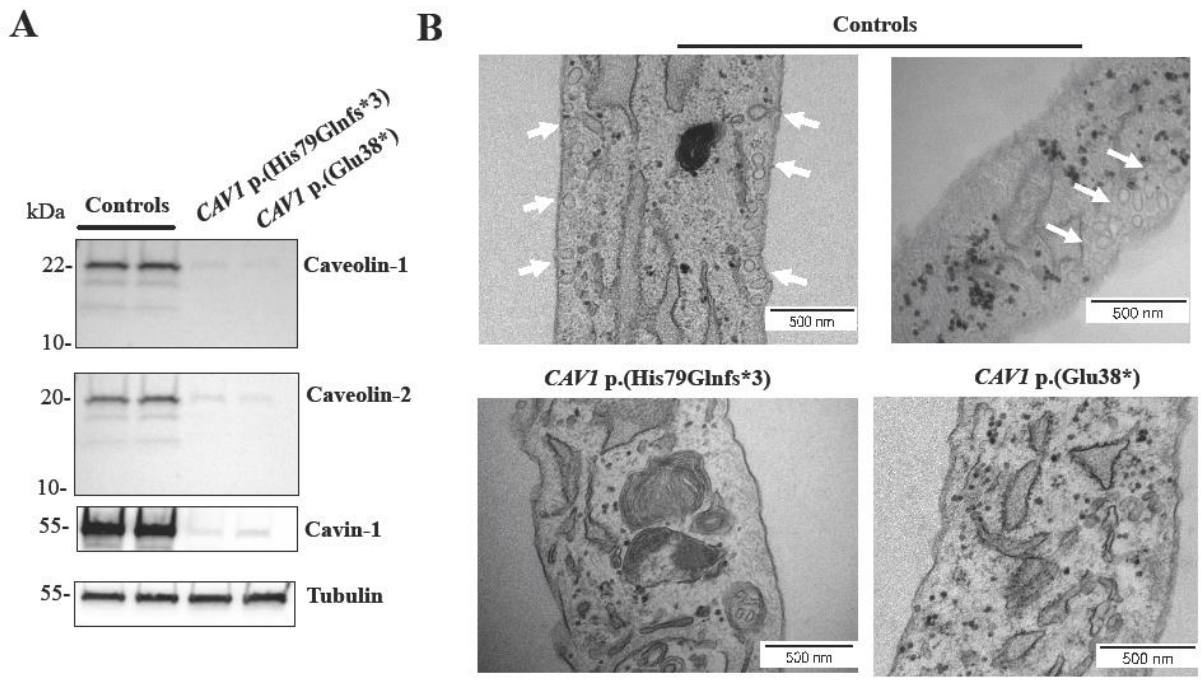

Figure 8. Homozygous *CAV1* null variants impair insulin signaling in patients' fibroblasts

(A) Insulin-mediated activation of insulin receptor ß-subunit (IRß), insulin receptor substrate-1 (IRS1), protein kinase B (AKT/PKB), and extracellular-regulated kinase (ERK)1/2 was evaluated by Western blot in fibroblasts from controls, from Patient 1, carrying the *CAV1* p.(His79Glnfs*3) homozygous pathogenic variant, and from the patient previously described

with a homozygous *CAV1* p.(Glu38*) variant responsible for CGL3 (9). Cells were maintained for 24h in a serum-free medium, then incubated or not with 50 nmol/L human insulin (#I9278, Sigma-Aldrich) for 8 min, and the total protein expression of signaling intermediates as well as their phosphorylated activated forms were evaluated. Representative images of Western blots performed in triplicate are shown. Tubulin is used as an index of the cellular protein level. Numbers on the left correspond to the expected protein molecular weight. (B) The effect of insulin on glycogen synthesis and (C) the ability of cells to bind insulin to its receptor, were evaluated as described in Methods. Results are expressed as the percentage of the first control without insulin. **: p <0.01, ns: not significant.

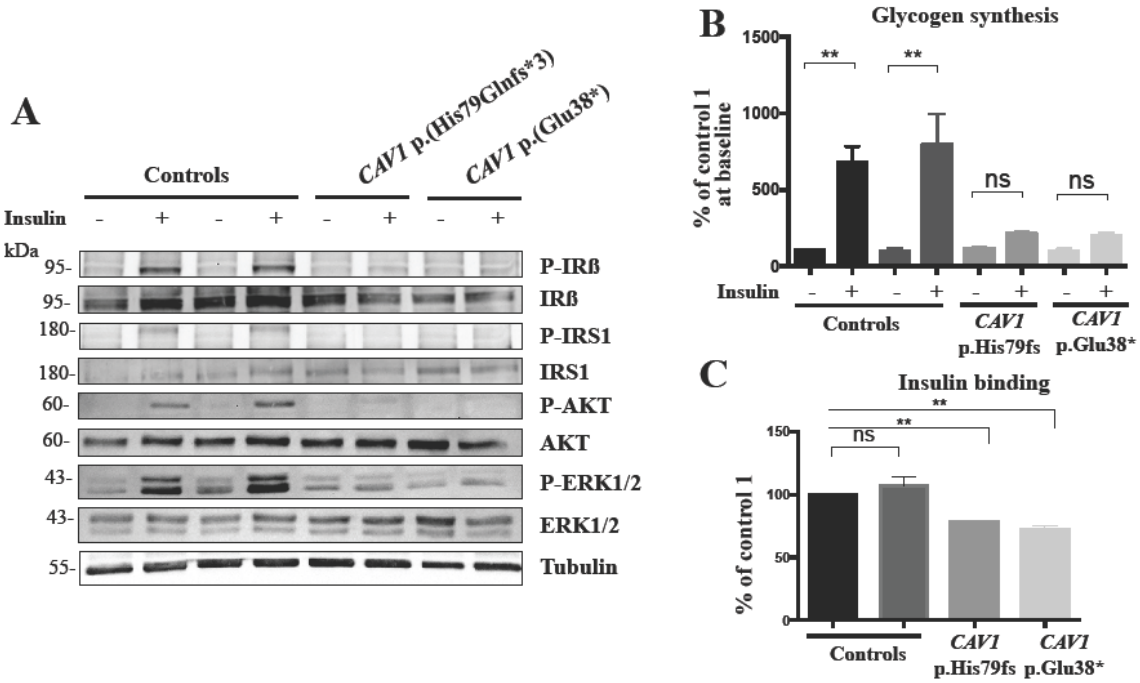

Figure 9. Homozygous *CAV1* null variants promote oxidative stress and senescence in patients' fibroblasts

(A) Reactive oxygen species (ROS) production was assessed by oxidation of 5-6-chloromethyl-2,7-dichlorodihydrofluorescein diacetate (CM-H_2DCFDA) in fibroblasts from controls, from Patient 1, carrying the *CAV1* p.(His79Glnfs*3) homozygous pathogenic variant, and from the patient previously described with a homozygous *CAV1* p.(Glu38*) variant

responsible for CGL3 (9). Results are normalized to DNA content measured by DAPI, and are expressed as the percentage of the first control. (B) Cellular senescence was evaluated by the protein expression levels of the cell cycle arrest and senescence protein markers p16, p21, and phospho-p53 as compared to total p53. Representative images of Western blots performed in triplicate are shown. Tubulin is used as an index of the cellular protein level. Numbers on the left correspond to the expected protein molecular weight. (C-D) Senescence-associated β-galactosidase activity (SA-β-gal) was assessed by X-gal staining at pH6 compared to non-specific staining at pH4. Representative immunofluorescence images from triplicate experiments are shown. Scale bar is 100 μm. The ratio of pH 6.0/pH 4.0 staining, which represents SA-β-galactosidase activity, is expressed as the percentage of the first control.

****: $p < 0.0001$, ns : not significant.

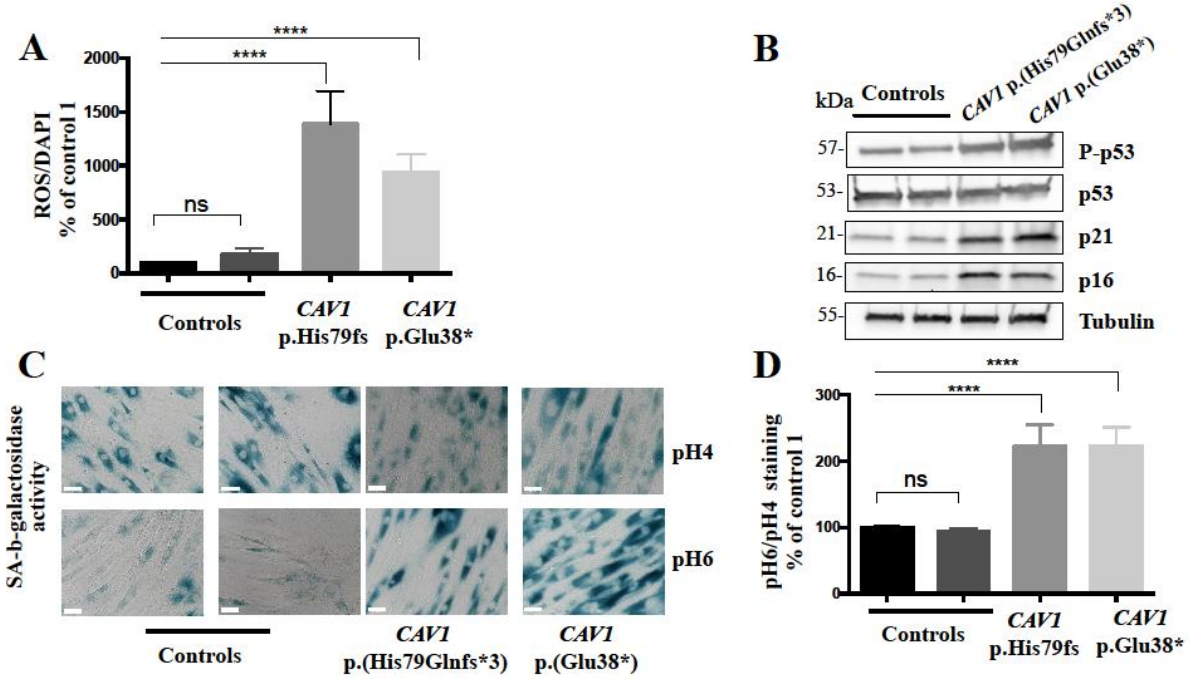

661 **Table 1. Main phenotypic features of Patients 1 to 4**
662

	Patient 1	**Patient 2**	**Patient 3**	**Patient 4**
Age at evaluation	15 years	18 years	10 years	8 months
Gender	Female	Male	Female	Female
Height (centile) (mid-parental target height in postpubertal patients)	153 cm (< 10^{th}) (160 cm)	155 cm (< 3^{rd}) (170 cm)	134 cm (< 25^{th})	62 cm (< 3^{rd})
Weight (kg) (centile)	42 kg (10^{th})	49 (3^{th})	30.5 (40^{th})	8.6 (75^{th})
Body Mass Index (kg/m^2) (centile)	17.9 (25^{th})	20.4 (25^{th})	17 (50^{th})	22.4 (ND)
Lipodystrophy onset	Early infancy	Early infancy	Early infancy	Early infancy
Generalized lipoatrophy sparing palms and soles	+	+	+	+
Failure to thrive in infancy	+	+	+	+
Increased appetite	+	-	-	-
Triangular face	+	+	+	+
Muscular hypertrophy	+	+	+	-
Acanthosis nigricans	+	+	-	-
Hirsutism	+	NA	-	-
Polycystic ovaries	+	NA	-	-
Liver steatosis (ultrasonography)	+	-	-	-
Blood pressure, cardiac examination and electrocardiogram	Normal	Normal	Normal	Normal
Echocardiography	Normal	Normal	ND	ND
Estimated right ventricular systolic pressure (N: 12-57 mmHg)	25	27	ND	ND
Megaesophagus	+	+	-	-
Muscular strength and neurological examination	Normal	Normal	Normal	Normal
Ophthalmological examination	Normal	**Atypical retinitis pigmentosa**	ND	ND
Fasting glucose (N: 3.5-5.6 mmol/L)	5.0	4.8	5.3	4.7
Fasting insulin (N: 2-9 mIU/L)	**300**	8.1	**9.6**	**9.4**
HbA1c (N: 4.8-6%)	5.8	5.3	5.4	5.1
Triglycerides (N: 0.3-1.5 mmol/L)	**5.4**	0.9	**3.4**	**2.3**
Total cholesterol (N: 3-5.1 mmol/L)	4.0	3.8	3.1	4.2
HDL-chol (N: 0.9-1.8 mmol/L)	**0.73**	**0.68**	**0.75**	**0.65**

Serum and urinary calcium	Normal	Normal	Normal	Normal
Urinary calcium/creatinine ratio (N < 0.14)	0.055	0.053	0.044	0.048
PTH (N : 15-65 pg/mL)	39.9	41.3	ND	ND
25-OH-Vitamin D (N: 50-200 nmol/L)	**28.2**	**23**	**34.4**	52.4
Bone mineral density (Lumbar spine Z-score)	**-2.78**	**-3.85**	ND	ND

The listed signs are indicated as present (+) or absent (-) in each patient.
NA, not applicable; ND, not determined
Height, weight and BMI centiles are determined according to CDC (Centers for Disease Control and Prevention, USA); Mid-parental target height is calculated according to Tanner *et al*. (44)

Supplemental Table 1

Antibodies used in Western Blot studies

Targeted protein	Source	Catalogue reference	Company	Dilution used
Primary antibodies				
Caveolin-1 (N-terminal part)	rabbit	sc-894	Santa Cruz Biotechnology (Dallas, TX, USA)	1:500
Caveolin-2	mouse	#610684	BD Biosciences (Franklin Lakes, NJ, USA)	1:1000
Cavin-1	rabbit	ab135655	Abcam (Cambridge, UK)	1:1000
Insulin receptor β (IRβ)	rabbit	#3025	Cell Signaling Technology (Danvers, MA, USA)	1:1000
Insulin receptor substrate 1 (IRS1)	rabbit	#17509-1-AP	Protein Tech (Rosemont, IL, USA)	1:1000
Phosphotyrosine residues	mouse	sc-7020	Santa Cruz Biotechnology	1:500
Total AKT	rabbit	#9272	Cell Signaling Technology	1:1000
Phospho-Ser473-AKT (P-AKT)	rabbit	#9271	Cell Signaling Technology	1:1000
Total extracellular signal-regulated kinase 1/2 (ERK1/2)	rabbit	#9102	Cell Signaling Technology	1:1000
Phospho-Thr202/Tyr204-ERK 1/2 (P-ERK)	rabbit	#9101	Cell Signaling Technology	1:1000
p53	mouse	#ab1101	Abcam	1:1000
Phospho-p53	rabbit	#ab38497	Abcam	1:1000
p21	rabbit	#10355-1-AP	Protein Tech	1:1000
p16	rabbit	#10883-1-AP	Protein Tech	1:1000
Tubulin	mouse	#T5168	Sigma-Aldrich (Saint-Louis, MO, USA)	1:1000
Secondary antibodies				
Rabbit IgG, horseradish peroxidase (HRP)-linked	goat	#7074	Cell Signaling Technology	1:3000
Mouse IgG, HRP-linked	horse	#7076	Cell Signaling Technology	1:3000